Third International Conference in Numerical and Experimental Aerodynamics of Road Vehicles and Trains (Aerovehicles 3)

Milan, Italy, June 13-15, 2018

Forcing three-dimensional large-scale flow asymmetries in the wake of a blunt body : wake equilibrium and drag reduction

Y. Haffner[1], J. Borée[1], A. Spohn[1], T. Castelain[2], M. Michard[3], S. Sesmat[4] and E. Bideaux[4]

Corresponding author : yann.haffner@ensma.fr

[1] Institut Pprime, UPR-3346 CNRS - ISAE-ENSMA - Université de Poitiers, Futuroscope Chasseneuil, France.

[2] Université de Lyon, Université Lyon 1, LMFA UMR CNRS 5509, 69622 Villeurbanne, France

[3] Université de Lyon, École Centrale de Lyon, LMFA UMR CNRS 5509, 69134 Ecully, France

[4] Laboratoire Ampère, Institut National des Sciences Appliquées de Lyon, Université de Lyon, 69621 Villeurbanne, France.

Abstract : We experimentally study the effect of high-frequency fluidic forcing on various asymmetric turbulent wakes behind a blunt body at $Re_H = 5 \cdot 10^5$. Different wake asymmetries are obtained by the use of passive perturbations around the body modifying the wake equilibrium. High-frequency forcing of the wake along the rear edges is then applied to increase the base pressure. Depending on the initial unforced wake vertical equilibrium, localized forcing along the top or bottom edges may strongly increase or decrease the base pressure. The efficiency of localized forcing and the fluidic boat-tailing thus created is linked to the global wake equilibrium and its modification.

Problem statement

The increasing need for energy saving in the land transport sector has brought many challenges for ground vehicles manufacturers to curb gas emissions, to face the depletion of fossil energy sources and to improve the range of green vehicles. As aerodynamic drag represents from one-third up to four-fifths of the vehicle's total energy consumption at highway speeds respectively for lorries and passenger cars, aerodynamics drag reduction is a key lever in the task of energy saving.

A plethora of drag reducing devices and techniques exist [1]. Passive techniques have the major drawback of being hardly applicable on finished car designs, already geometrically optimized. One solution is the design of active flow control solutions using fluidic devices such as pulsed jets in order to modify the flow without changing the vehicle geometry.

Such techniques have been proven efficient for reducing the wake drag of simplified car geometries. Using tangentially pulsed jets near flow separation at moderate free-stream flow velocities [2] managed to significantly reduce the base drag of a square-back Ahmed body. This was achieved through the use of high frequency forcing decoupled from the natural instabilities of the wake allowing to promote a fluidic boat-tailing effect.

The wake of such simplified square-back body is very sensitive to different geometrical modifications such as localized passive perturbations around the body [3], in particular underbody-flow changes [4], resulting in various wake dynamics and topologies. One of the main features of such wakes is the presence of large-scale asymmetries impacting the base pressure distribution, manifesting either as static asymmetries or bi-modal asymmetries.

The present work aims at investigating the effect of high-frequency fluidic forcing on perturbed wake symmetries of a square-back Ahmed body. We study how global forcing along all the back edges or localized forcing along only some edges interacts with the unforced wake asymmetries and how it modifies the base pressure distribution and the drag.

Experimental setup

The experimental setup used for this study is presented in figure 1. A blunt body similar to a square-back Ahmed body is placed on a false floor containing a 6-components aerodynamic balance to measure aerodynamic loads. The back pressure is monitored using a series of pressure taps linked to a pressure scanner (for time-averaged measurements) and to differential pressure sensors (calibrated for time-resolved measurements). Large-scale PIV measurements are performed to investigate the wake flow in the vertical plane of symmetry of the body. Free-stream velocity in the wind-tunnel is fixed at $U_0 = 25\text{m/s}$ corresponding to a Reynolds number based on the height of the body of $Re_H = 5 \cdot 10^5$.

In order to perturb the wake asymmetries of the unforced flow, we use cylinders of diameter $d = 0.053H$ and $0.067H$, placed spanwise either over or under the body, one height H upstream the rear edge. The asymmetry of the wake flow is characterized using 4 pressure taps on the back to estimate the vertical $\delta_{pz} = C_p(T) - C_p(B)$ and lateral $\delta_{py} = C_p(L) - C_p(R)$ pressure gradients.

Actuation is performed using pulsed jets generated by an ensemble of solenoid valves supplied with compressed air and linked by semi-rigid tubing to diffusers ending in $h = 1\text{mm}$-thick slits. The slits from all 4 edges can be driven independently in order to perform actuation only on selected edges or with different actuation commands depending on the edges. A curved surface of radius $r = 9h$ is placed at the base of the slits in order to promote flow deviation. In the frame of the present study, actuation is performed at a high frequency, decoupled from the natural instabilities of the wake (namely global vortex shedding and shear layers convective instability), with corresponding Strouhal number based on U_0 and the boundary-layer momentum thickness θ at the top separation $St_\theta = 0.096$, with varying momentum coefficient C_μ.

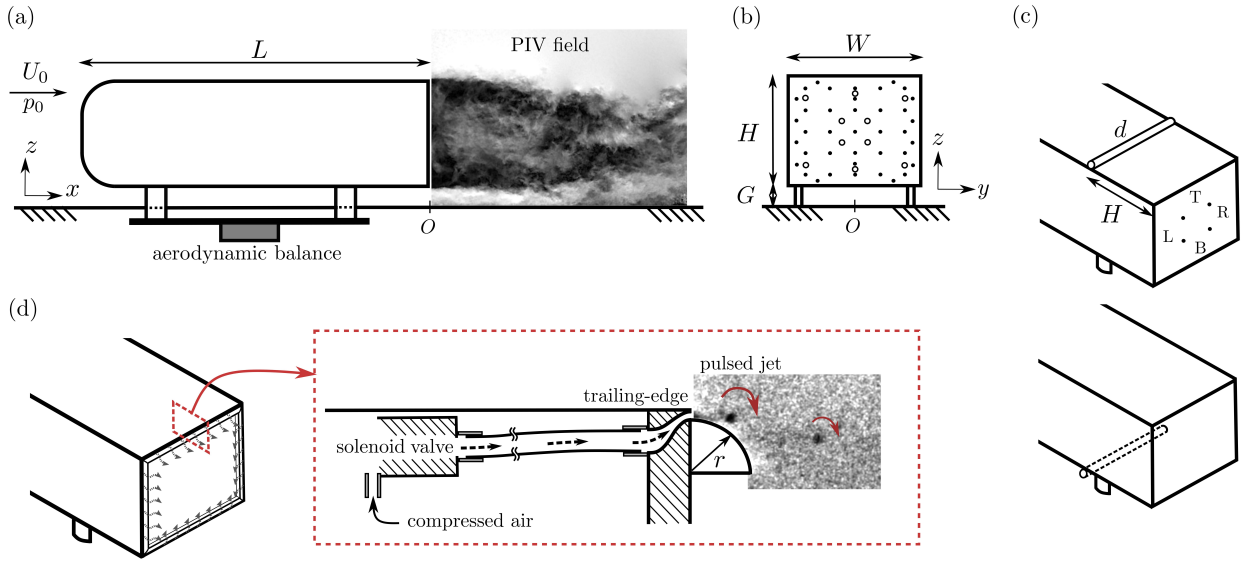

Figure 1: Experimental setup. (a) Side-view of the bluff body geometry studied : detail of the PIV field-of-view in the wake and of the balance setup to measure aerodynamic loads. (b) Rear-view : pressure taps locations used for wall pressure measurements at the back. (c) Perturbation of the flow equilibrium using spanwise cylinders of diameter d localized in either top or bottom boundary layer. (d) Actuation setup : forcing by pulsed jets along the rear edges, and detailed view of the pulsed jets generation with a visualization of small-scale vortical structures exiting the slits as regions with a strong deficit of particles.

Results

We study three different unforced wake configurations by perturbing either the top or bottom of the body. The corresponding wake topologies are highlighted in figure 2 and the corresponding main global aerodynamic characteristics are given in table 1. The natural unperturbed wake is characterized by a vertical equilibrium and horizontal bi-modal behaviour, and exhibits the highest mean base pressure coefficient C_{pb} (associated with lowest drag). Perturbations localized on top and bottom of the body result in vertically statically asymmetric wakes respectively with a negative and positive vertical pressure gradient δ_{pz}. These vertically asymmetric states are characterized by the predominance of either the top or bottom shear layer in the formation process of the wake through fluid entrainment from the external region of the flow.

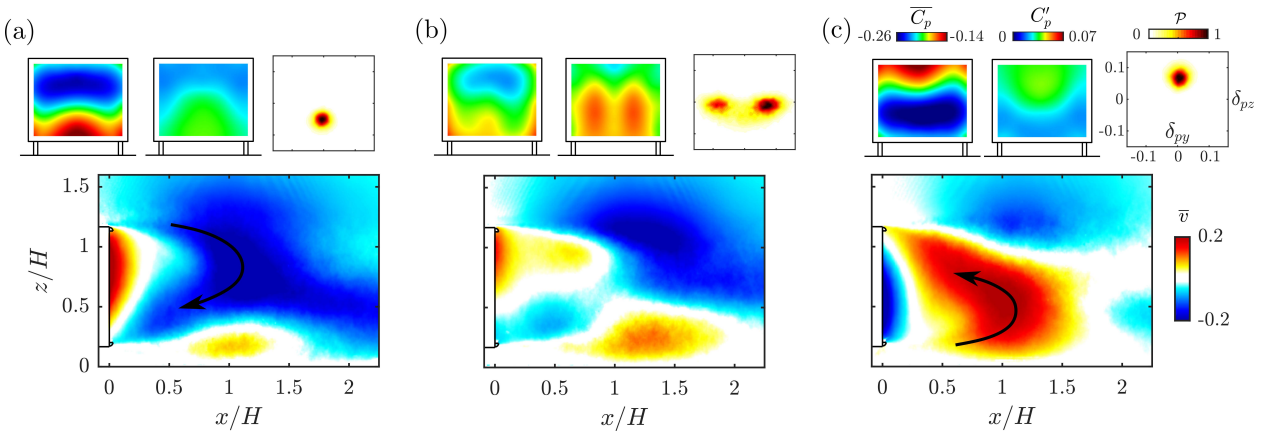

Figure 2: Unforced wake flow topologies depending on the localization of the cylinder perturbation. (a) Perturbation in the top boundary layer. (b) Natural unperturbed flow. (c) Perturbation in the bottom boundary layer. Top, from left to right are respectively the time-averaged $\overline{C_p}$ distribution at the back, the fluctuations of C_p, and the probability distribution of the back pressure gradient $\mathcal{P}(\delta_{py}, \delta_{pz})$. Bottom is the mean vertical velocity field $\overline{v}$: arrows sketch the main entrainment motion forming the recirculation region.

Perturbation	$\overline{C_{pb}}$	C_L	$\overline{\delta_{pz}}$
—	-0.196	-0.12	-0.009
Top	-0.209	-0.077	-0.052
Bottom	-0.215	-0.126	0.068

Table 1: Aerodynamic characteristics of the three unforced flow configurations : mean base pressure coefficient $\overline{C_{pb}}$, lift coefficient C_L and mean vertical base pressure gradient.

Two major questions arise from these observations : 1—How these different wakes react to global and localized forcing and 2—If starting from a vertically asymmetric wake, can we achieve a marginal additional drag decrease by symmetrizing the wake.

In order to address these questions, we perform on these three wakes different spatially localized actuations by selecting either all the edges, only the top and lateral edges or only the bottom and lateral edges.

Figure 3 presents the effect of these various forcing conditions on the base pressure parameter $\gamma_p = \overline{C_{pb}}/\overline{C_{pb}}_{\text{unforced}}$. Global forcing along all edges results in a robust $\sim 20\%$ base pressure increase ($\gamma_p < 1$) corresponding to $\sim 9\%$ of drag decrease without changing noticeably the wake equilibrium no matter the unforced flow state. An important pressure recovery saturation appears at higher forcing amplitudes.

On another hand, localized forcing leads to very different results depending on the unforced flow asymmetry. Interestingly, vertically static asymmetric states can be forced on the side of the highest pressure region at the back with almost as much efficiency in drag reduction as global forcing. This drag reduction seems to depend on the degree of vertical asymmetry of the unforced flow when comparing results of localized forcing on both vertically asymmetric wakes.

Conversely, forcing on the opposite side leads to more moderate drag reductions up to a given forcing amplitude C_μ above which drag recovery starts to deteriorate and wake asymmetry is further increased.

For the natural vertically symmetric wake, localized forcing leads in all cases to very moderate drag reductions. This observation is concomitant with a modification of the vertical wake equilibrium and an important sensitivity of this equilibrium to localized forcing. Once vertical symmetry is broken, drag deteriorates noticeably as the forcing amplitude is increased. These observations suggest that the effect of fluidic boat-tailing as a base pressure recovery mechanism and the global equilibrium of the wake are intimately linked.

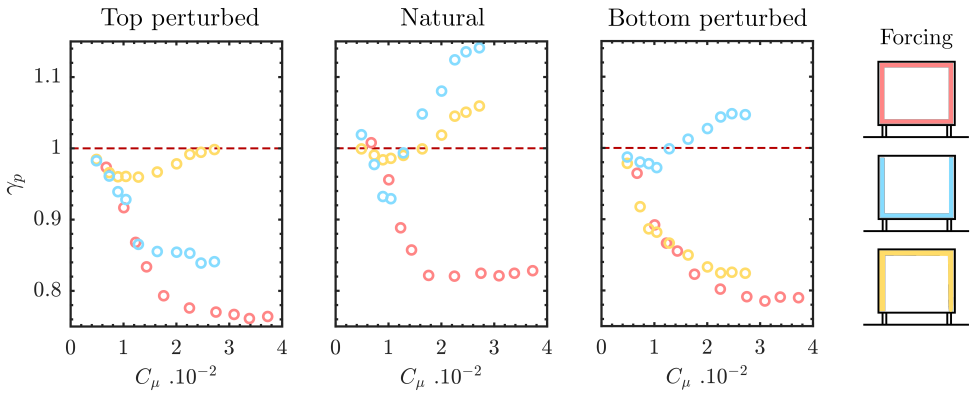

Figure 3: Effect of localized high-frequency forcing on the integrated base pressure coefficient depending on the unforced flow symmetry. Sketches on the right indicate which edges are used to force the wake. Red dashed line distinguishes between base pressure recovery ($\gamma_p < 1$) and base pressure decrease ($\gamma_p > 1$).

Further wake flow analysis will present in detail the relation between forcing effect, global wake equilibrium and drag changes. Additionally, investigation of asymmetric forcing effects on restoring the vertical symmetry of perturbed wakes will be discussed.

Acknowledgements

The authors acknowledge the funding of the program Activ_ROAD (ANR-15-CE22-0002) by the French Agence Nationale de la Recherche (ANR). We thank other members of the program for insightful discussions and valuable contributions : J. M. Breux, D. Chacaton, L. Cordier, F. Harambat, B. Noack, F. Paillé and C. Sicot. We also thank the implication of our industrial partners PSA Group and Renault Trucks in the program.

References

[1] H. Choi, J. Lee, and H. Park. Aerodynamics of heavy vehicles. *Ann. Rev. Fluid Mech.*, 46:441–468, 2014.

[2] D. Barros, J. Borée, B. R. Noack, A. Spohn, and T. Ruiz. Bluff body drag manipulation using pulsed jets and coanda effect. *J. Fluid Mech.*, 805:422–459, 2016.

[3] D. Barros, J. Borée, O. Cadot, A. Spohn, and B. R. Noack. Forcing symmetry exchanges and flow reversals in turbulent wakes. *J. Fluid Mech.*, 829:R1, 2016.

[4] M. Szmigiel. *Etude du flux de soubassement sur la dynamique du sillage d'un corps non profilé à culot droit : Application du contrôle actif pour la réduction de trainée de véhicule industriel.* PhD thesis, Ecole Centrale de Lyon, 2017.